Catalysis Today 180 (2012) 105–110

Contents lists available at ScienceDirect

Catalysis Today

journal homepage: www.elsevier.com/locate/cattod

Preferential oxidation of CO (CO-PROX) over CuO_x/CeO_2 coated microchannel reactor

O.H. Laguna [a,*], E.M. Ngassa [a], S. Oraá [a], A. Álvarez [a], M.I. Domínguez [a], F. Romero-Sarria [a], G. Arzamendi [b], L.M. Gandía [b], M.A. Centeno [a], J.A. Odriozola [a]

[a] Departamento de Química Inorgánica e Instituto de Ciencia de Materiales de Sevilla, Centro Mixto Universidad de Sevilla-CSIC, Avenida Américo Vespucio 49, 41092 Seville, Spain
[b] Departamento de Química Aplicada, Edificio de los Acebos, Universidad Pública de Navarra, Campus de Arrosadía s/n, E-31006 Pamplona, Spain

ARTICLE INFO

Article history:
Received 20 December 2010
Received in revised form 17 February 2011
Accepted 6 March 2011
Available online 9 April 2011

Keywords:
Microchannel reactor
CO-PROX
Computational fluid dynamics (CFD)
CuO_x/CeO_2
Process intensification

ABSTRACT

The general aspects of the synthesis and characterization results of a CuO_x/CeO_2 catalyst were presented. In addition the principal steps for manufacturing a microchannel reactor and for the coating of the CuO_x/CeO_2 catalyst onto the microchannels walls, were also summarized. The catalytic activity of this microchannel reactor during the preferential oxidation of CO (CO-PROX) was evaluated employing a feed-stream that simulates a reformate off-gas after the WGS unit. Two activation atmospheres were studied (H_2/N_2 and O_2/N_2). The reducing pretreatment improved the resistance to deactivation by formation of carbonaceous species over the catalyst surface at high temperatures. The presence of H_2O and CO_2 in the feed-stream was also analyzed indicating that the adsorption of CO_2 inhibited the conversion of CO at lower temperatures because these compounds modified the active sites through the formation of carbonaceous species on the catalyst surface. Finally, the experimental results of the microreactor performance were compared with CFD simulations that were carried out using a kinetic for the CuO_x/CeO_2 powder catalyst. The experimental results were reasonably well described by the model, thus confirming its validity.

1. Introduction

The current interest in finding alternative energy sources has allowed the development of different researches focused on the transformation of hydrogen for the production of electricity [1]. This is an attractive process especially from a environmental point of view, however the real ecologic impact of H_2 as an energy carrier is in the processes involved in its production. Considering that hydrogen is not an isolated element, it has to be extracted from organic molecules such as hydrocarbons, alcohols or ethers through reforming processes and consequently CO_2, H_2O and CO are also produced [2,3].

The low-temperature polymer-electrolyte-membrane fuel cells (PEMFCs) that convert hydrogen to generate electricity require high-purity hydrogen as fuel. Specially, the CO content in the feed must be limited to 10 or 100 ppm, depending on the anode composition. For that reasons, after the reforming processes additional purification steps are needed and the high and low-temperature water-gas shift (WGS) processes have been widely applied. Nevertheless, the CO contents leaving the WGS units can be between ca. 0.5% and 2 vol.%, being still required CO removals to trace levels [4]. In this regard, the preferential oxidation of CO (CO-PROX) is being considering taking into account its effectiveness. This reaction takes place at atmospheric pressure and low temperatures, which allows reducing the influence of the reverse water-gas shift r-WGS reaction [4]. For the CO-PROX reaction, several catalysts have been checked [5] and one of the most studied solids is the mixed system Cu–Ce. This system presents good CO conversion and CO oxidation selectivity levels depending on the Ce–Cu interaction that can be influenced by the copper content and the synthesis conditions [6]. On the other hand, this solid is attractive for industrial applications because of its low cost compared to the noble metal-based catalysts [7,8].

The integration of the hydrogen production and purification processes is being routed to portable and automotive applications where the PEMFCs can be incorporated. Conventional packed-bed reactors have several drawbacks such as pressure drop, temperature gradients, and risk of hot spot formation due to the high exothermicity of the oxidations of CO and H_2. In this sense, microreactors have advantages such as fast response time, easy integration and small footprint, which are ideal for portable systems. Additionally, these devices present good mass and heat transport properties [9,10].

The study of microreactors for different reactions is currently growing and several reports can be found in the literature. In the case of the CO-PROX reaction, Kolb et al. [11] and O'Connell

* Corresponding author. Tel.: +34 954489221; fax: +34 954460665.
E-mail address: oscarh@icmse.csic.es (O.H. Laguna).

0920-5861/$ – see front matter © 2011 Elsevier B.V. All rights reserved.
doi:10.1016/j.cattod.2011.03.024

et al. [12] have reported on the CO-PROX reaction performed in a microstructured reactor. The system reduced the CO levels from 1% in the feed to 25–60 ppm at the microreactor outlet. On the other hand, Dudfield et al. [13] operated a compact fin heat-exchanger reactor containing 2.5% Pt–Ru catalyst for the same reaction. Divins et al. [14] reported the functionalization with Au/TiO_2 of a silicon microreactor containing ca. 40,000 regular channels of 3.3 μm in diameter per square millimeter for the CO preferential oxidation. They demonstrated that the performance in the CO oxidation of the silicon microreactor was better than showed by other systems obtained over a conventional cordierite with 400 cpsi that were loaded with the same catalyst.

In addition to the issues involved in the presented scenario, the modeling and simulation of microreactors should be also considered. The principal aim of the modeling is to obtain information for the understanding of the system and consequently to be able to predict its behavior. The formulation of the models requires the consideration of transport phenomena, thermodynamic and kinetic aspects involved in the chemical and physical process during the reaction. In this regard, the simulation and modeling based on computational fluid dynamics (CFD) have attracted increasing interest and have been successfully applied to the analysis and design of micro-flow devices [15] and catalytic microreactors [16–18].

In the present work the synthesis of a CuO_x/CeO_2 catalyst, the manufacturing of a microchannel reactor and the coating of the microchannels walls with the powder catalyst are summarized. In addition the catalytic performance of the microreactor during the CO-PROX reaction is presented, analyzing the effect of the catalyst activation prior to the reaction and the influence of the presence of H_2O and CO_2 in the feed-stream. Finally the experimental results of the CO conversion and CO oxidation selectivity are compared with the simulations using the model previously formulated for the microchannel reactor containing the CuO_x/CeO_2 as the coated catalyst.

2. Materials and methods

2.1. Synthesis and characterization of the CuO_x/CeO_2 powder catalysts

The synthesis of the CuO_x/CeO_2 catalyst by coprecipitation method was reported in a recent work [19]. Two aqueous solutions (0.5 M) of $Cu(NO_3)_2$ and $Ce(NO_3)_3$ were mixed under vigorous stirring, to get 9:1 $Ce(OH)_3$:$Cu(OH)_2$ weight ratio, then a NaOH solution (2 M) was added dropwise until a stable pH of 9 was reached. A precipitate with the mixture of Cu and Ce hydroxides was generated. This solid was filtered and washed with distilled water; dried overnight at 60 °C and finally, calcined at 300 °C for 2 h.

The obtained material was characterized by means of X-ray fluorescence (XRF), N_2 adsorption (BET specific surface area), X-ray diffraction (XRD), Raman spectroscopy and temperature programmed reduction (TPR). The results were presented in our recent reports [19,20]. As the most relevant features of this catalyst it can be mentioned that it presented a copper content of 15 wt.% (expressed as $Cu(OH)_2$). The BET specific surface area was 76 m^2/g and the XRD analysis showed the characteristic pattern of the c-CeO_2 fluorite structure [5,21,22]. The presence of copper species did not modify the diffraction lines of CeO_2. Additional reflections associated with the presence of copper oxides were not detected and this result was correlated with the high dispersion of the copper species over the CeO_2 surface [19].

As for the Raman spectroscopy, the most important feature was that the oxygen vacancies signal (at 612 cm^{-1}) increased upon heating due to the dehydroxylation of the catalyst surface. This was important because the formation of oxygen vacancies promoted the oxygen mobility in the CeO_2 structure [19].

The TPR profile showed two main reduction processes at high and low-temperature. Two peaks centered at 727 °C and 854 °C represented the high-temperature reduction of the Ce^{4+} cations in the bulk of the material [23]. The peak centered at 184 °C was due to the low-temperature reduction of some surface Ce^{4+} cations and the reduction of all the Cu^{2+} cations, thus demonstrating the synergy between the two elements [19,24,25].

2.2. Microblock manufacturing and coating with the CuO_x/CeO_2 catalyst

The details about the manufacturing process were recently published by Cruz et al. [19]. This device was manufactured using Al-alloyed ferritic stainless steel (Fecralloy®) [19,26–28]. Microchannels were fabricated by micro-milling 1 mm thick ferritic stainless steel plates that were joined together using the transient liquid phase (TLP) bonding process using a nickel-based interlayer with a composition of Ni–14B–7Si (wt.%, Goodfellow). A bonding temperature of 850 °C with an applied force of 2.8 kN (~7 MPa) was selected [29]. The TLP bonded samples were finally treated at 1200 °C for 5 h.

Micromachining and joining of the steel plates resulted in a microblock that was housed in Al-alloyed ferritic steels cases (Fig. 1) after the coating process of the catalyst onto the walls of the microchannels. Previously, the surface of the microchannel block was modified generating a surface oxide layer that enhanced the adhesion of the catalyst upon heating in air at elevated temperatures [26–28]. Upon heating at 900 °C for 22 h in air the microchannel block, an homogeneous surface layer of Al_2O_3 was formed, presenting the needle-like structure of the formed whiskers [19].

The washcoating process was selected for coating the microchannels with the CuO_x/CeO_2 catalyst using a slurry with the following composition: 76 wt.% powder CuO_x/CeO_2 catalyst, 7 wt.% polyvinyl alcohol (PVOH) and 17 wt.% colloidal alumina. The pH of the suspension was adjusted to 4 with diluted HNO_3 [19,30,31]. The use of HNO_3 gave rise to the leaching of copper species resulting in a decreasing of about 50% of the original CuO loading. The leaching of copper species presumably generated a higher BET surface area of the dried slurry (92 m^2/g) compared with that of the CuO_x/CeO_2 catalyst (76 m^2/g) [19].

Once the microchannels were immersed in the slurry, the elimination of excess was done by air blowing (2 L/min). After each coating process, the microchannel block was dried at 120 °C for 30 min and finally the microblock was calcined at 300 °C for 3 h (1 °C/min). This method resulted in a microchannel block loading of 5.46 mg/cm^2 after eight washcoating processes, with a total load of 300 mg of catalyst [19].

2.3. Catalytic activity measurements

The CO-PROX reactions were carried out at atmospheric pressure in a PID Eng&Tech Microactivity set-up that allowed the setting up of the assembled microchannel reactor. This equipment allows the programming and monitoring of the process variables such as temperature, flow of the gases and the analysis time. Different temperatures were evaluated and these were monitored by 4 K-type thermocouples, two at the inlet and the outlet of the microblock and the other two were placed in lateral walls of the microblock. The temperature of reaction was taken as the average between the inlet and the outlet temperatures.

Prior to the reactions, the catalyst was activated under reducing or oxidizing conditions (depending on the experiment) with 30 mL/min of 21% H_2 or O_2 respectively, in N_2 for 3 h at 300 °C. For the experimental runs, a stream with 300 mL/min (STP) of total flow-rate was used. The feed stream composition was set at: 1 vol.%

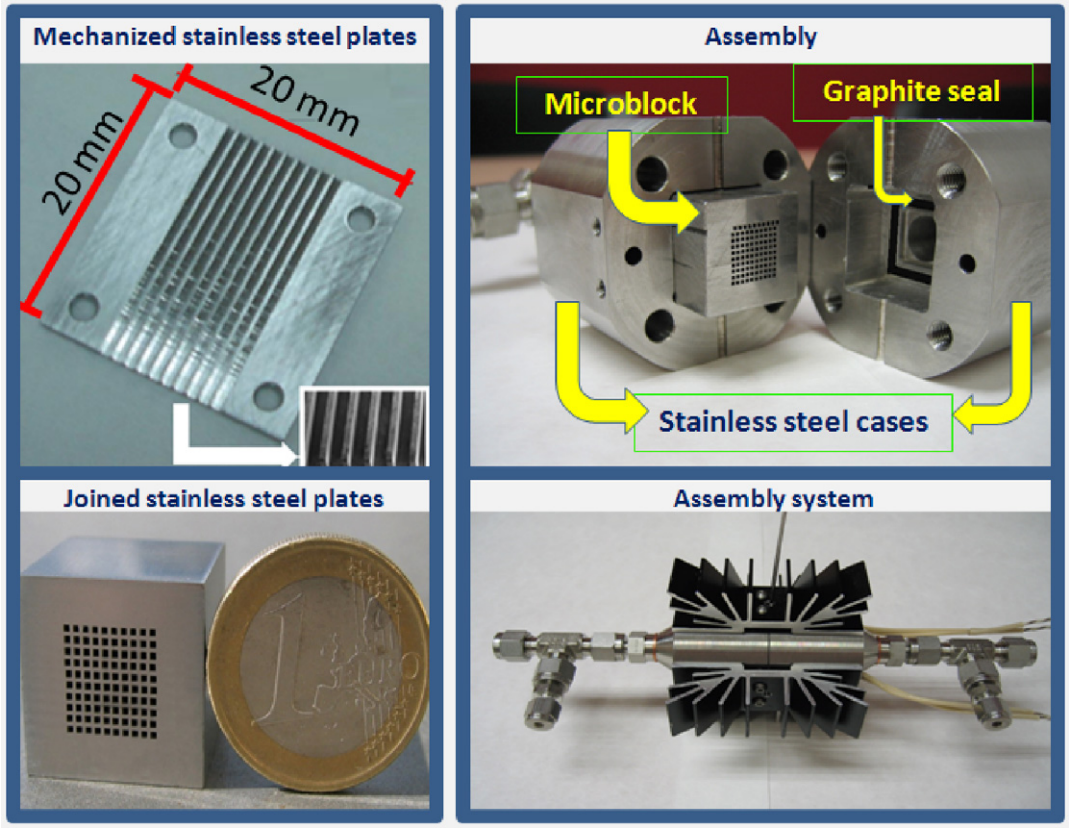

Fig. 1. Assembling of the microchannel reactor for the CO-PROX reaction.

CO, 2 vol.% O_2, 10 vol.% CO_2, 10 vol.% H_2O, 70 vol.% H_2 and N_2 as balance to simulate a reformate off-gas after the WGS unit [20]. For studying the influence of the presence of CO_2 and H_2O in the flow during the PROX reaction, a series of catalytic runs with different stream compositions (Table 1) were tested.

Product and reactants were analyzed by online gas chromatography (Agilent® 7890 equipped with a Porapak® Q, two Molecular Sieve 5A, and two Hayesep® Q columns) and then quantified using a TCD detector. The CO conversion and the CO oxidation selectivity were calculated according to [5].

$$\text{CO conversion}\ (\%) = \frac{(CO_{in} - CO_{out}) \times 100}{CO_{in}} \quad (1)$$

$$\text{CO oxidation selectivity}\ (\%) = \frac{(CO_{in} - CO_{out}) \times 100}{2(O_{2_{in}} - O_{2_{out}})} \quad (2)$$

2.4. Microrreactor models and simulations conditions

A detailed description of the mathematical model used for analyzing the experimental results was presented recently by Arzamendi et al. [20]. Three-dimensional simulations have been carried out using ANSYS CFX software which is based on the finite-volume method for spatial discretization of the Navier–Stokes equations. Simulations were performed on a Dell Precision PWS690 workstation running MS Windows XP® x 64 with an available RAM of 16.0 GB.

The model consisting of square parallel microchannels of 20 mm of length and 0.70 mm of side was previously developed and it has been successfully applied to study the steam reforming of methane and methanol [16,17]. This model has three main physical domains, two of them are fluidic and the other corresponds to the solid block (stainless steel). These domains were meshed using prismatic and hexahedral elements resulting in dense computational unstructured grids [16,17,20].

CFD simulations have been conducted at steady state conditions and isothermal conditions. It has been assumed that a thin layer of the catalyst was uniformly deposited onto the walls of the microchannels with a loading of 5.46 mg/cm^2. The feed-stream composition was set as the real data recorded by the chromatographic analysis for all gases.

Catalytic reactions were modeled considering the microchannels walls as sources of products and sinks of reactants [16,17,20]. A reaction scheme including the oxidation of CO to CO_2, the oxidation of H_2 to H_2O and the r-WGS reaction has been considered. The kinetic equations implemented in the code for the CFD simulations were taken from a kinetic study carried out over the CuO_x/CeO_2 powder catalyst [20].

Table 1
Feed stream compositions of the catalytic tests for the study of the influence of CO_2 and H_2O.

	CO vol.%	O_2 vol.%	H_2 vol.%	CO_2 vol.%	H_2O vol.%	N_2 vol.%
Composition 1	1	2	70	0	0	27
Composition 2	1	2	70	0	10	17
Composition 3	1	2	70	10	0	17
Composition 4	1	2	70	10	10	7

3. Results and discussion

3.1. Catalytic activity of the microchannel reactor

3.1.1. Influence of the activation treatments

As indicated above, the CO-PROX reaction was carried out after two different activation treatments. The first one was achieved under reducing conditions (with H_2) and the second one employing

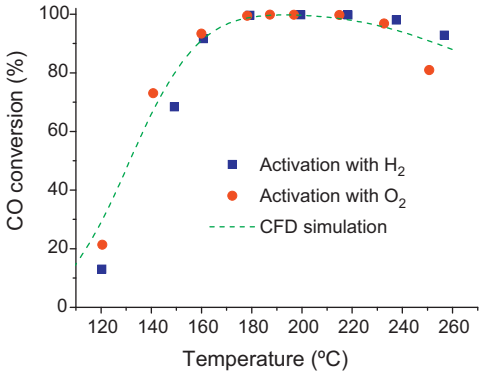

Fig. 2. CO conversion (effect of the activation treatment prior to the CO-PROX reaction and comparison with the isothermal CFD simulation).

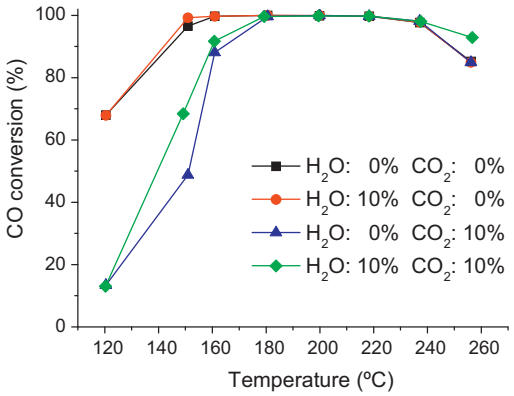

Fig. 4. CO conversion (influence of the presence of H_2O and CO_2 in the feed-stream).

O_2. The results of the CO conversion and the CO oxidation selectivity are presented in Figs. 2 and 3 respectively.

After the two pretreatments, the experimental results show that the CO conversion increases with the temperature reaching a maximum (close to 100%) between 180 °C and 220 °C. No significant differences can be inferred from the two activation processes and the catalytic activity is almost the same in both cases.

The catalytic activity of the reduced catalyst is in agreement with that in our reports where the catalytic activity of the CuO_x/CeO_2 catalyst during the CO-PROX reaction was closely related to the presence of metallic copper [19,20]. The similar results of the oxidized catalyst at lower temperature are suggesting that probably the Cu^+ or Cu^{2+} species have a considerable catalytic activity as was proposed previously in different works [32,33]. The Cu^+ and Cu^{2+} cations can act as preferential positions for the adsorption of CO molecules, being especially active those copper ions that are in close contact with the CeO_2 matrix. Martínez-Arias and coworkers proposed that CO reduces the catalyst surface upon adsorption over the Cu^{2+} species and promotes the formation of oxygen vacancies in the CeO_2 matrix [34].

However, the TPR profile of the CuO_x/CeO_2 solid that is coated onto the microchannels showed that the low-temperature reduction started at temperatures that are very similar to the lowest temperatures that are studied during the PROX reaction. If it is considered and that the feed-stream of the CO-PROX reaction has a higher reducing character owing to its high H_2 content (70 vol.%), it can be expected that even for the previously oxidized catalyst, the copper species are reduced rapidly during the beginning of the reaction.

At the highest temperature considered in this work, the reduced catalyst presents a higher catalytic activity than the oxidized one.

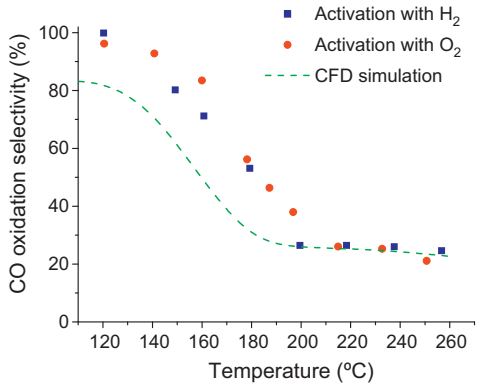

Fig. 3. CO oxidation selectivity (effect of the activation treatment prior to the CO-PROX reaction and comparison with the isothermal CFD simulation).

Although the difference is small, this behavior could be suggesting a higher stability of the carbonaceous species adsorbed onto the surface for the oxidized catalyst. It seems likely that the formation of the carbonaceous species is promoted as temperature increases; however, it should be pointed out that in the case of the reduced catalyst the adsorption of carbonaceous species is less stable. As a result, a lower tendency to deactivation is shown for the reduced catalyst.

The CO oxidation selectivity (Fig. 3) decreases as the temperature increases and no differences can be established regarding the two pretreatments. The general trend in both cases indicates that as the temperature increases the H_2 consumption is promoted. This is in agreement with our kinetic study over the CuO_x/CeO_2 powder catalyst during the CO-PROX reaction [20]. The activation energy of the H_2 oxidation (110 kJ/mol) is considerably higher than that of CO oxidation (36.9 kJ/mol) and this is the reason for the good CO oxidation selectivity at low temperatures.

3.1.2. *Effect of the presence of H_2O and CO_2 in the feed-stream*

Considering that the activation under H_2/N_2 flow generated a slightly better catalytic performance at higher temperatures (Fig. 2), this pre-treatment was selected for the evaluation of the effect of the presence of H_2O and CO_2 in the feed-stream. A series of catalytic runs were carried out after the reducing treatment with four different compositions of the feed-stream (Table 1) and the CO conversion results are presented in Fig. 4.

The feed-stream without H_2O and CO_2 gives similar results than the reaction carried out with the addition of 10 vol.% H_2O. In both cases the CO conversion is higher than in the two reactions with CO_2 in the feed-stream. The CO_2 makes difficult the CO oxidation at low temperatures (between 120 °C and 180 °C) whereas H_2O does not generate a considerable effect. This suggests that over this catalyst the CO conversion is not strongly influenced by side reactions as the WGS or r-WGS at low temperatures.

As concerns the catalytic runs in which CO_2 was present in the feed-stream, these compound may be adsorbed onto active sites that in the case of the reduced catalyst have to be associated with surface metallic copper. At temperatures above 180 °C this adsorption is less favored, thus enhancing the probability of the interaction between the CO molecules and the active sites and consequently promoting their oxidation. For these experiments, the main differences can be observed between 140 °C and 150 °C and this can be associated with the presence of H_2O. The experiment with H_2O shows higher CO conversion near to 150 °C. Probably there is an interaction between H_2O and the adsorbed carbonaceous species onto the catalyst surface modifying their symmetry and probably making them more labile. This is allowing the desorption of the carbonaceous species at lower temperatures [35] than in the case of the catalytic run where H_2O is not present in the feed-stream.

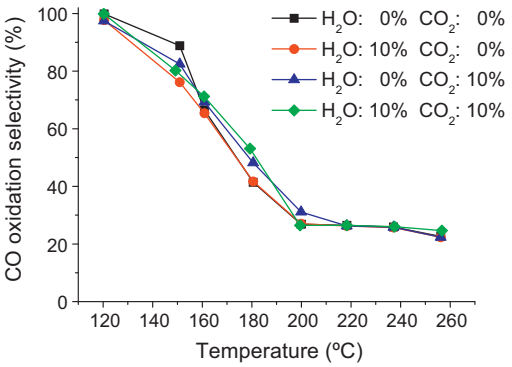

Fig. 5. CO oxidation selectivity (influence of the presence of H_2O and CO_2 in the feed-stream).

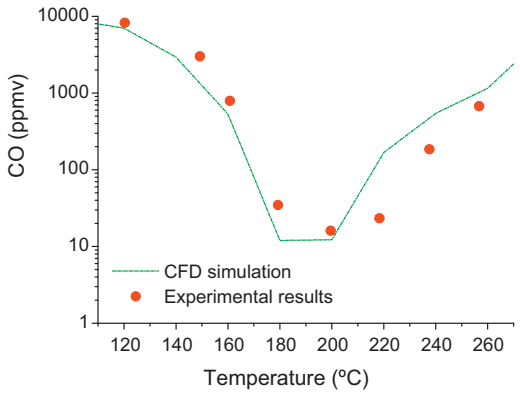

Fig. 6. CO concentration at the microchannel outlet (comparison between the experimental results and the isothermal CFD simulation).

The CO oxidation selectivity (Fig. 5) does not present differences among the four experiments. The decrease of the CO oxidation selectivity as the temperature increases is confirmed for all cases. When CO_2 is present in the feed-stream, although the number of CO molecules converted is lower at temperatures below 180 °C, this does not mean that the H_2 oxidation has been promoted. This is confirming that the relatively low activation of the CO oxidation favors this reaction even with the presence of CO_2 molecules that can be blocking the active sites at the surface of the catalyst. This could be complemented with the fact that there is little influence of H_2O on the side reactions as WGS or r-WGS in this case.

3.1.3. Comparison between the experimental results and the isothermal CFD simulations

A first comparison between the model and the experimental results is presented in Fig. 2. The CO conversion trends after the two types of activation processes, that presented a very similar behavior, are well described by the applied model. This is relevant result because it validates the mathematical model previously developed for the microchannel reactor that includes the kinetic model obtained with the CuO_x/CeO_2 powder catalyst. Accordingly, diffusional effects in the catalyst layer can be neglected. As regards the kinetic model this is confirming that not only the CO and H_2 oxidation must be considered but also the r-WGS, which is a side reaction that influences the CO-PROX kinetics [20,36]. In addition, this is pointing out that after the washcoating process the catalytic properties of CuO_x/CeO_2 remain virtually unaltered.

At the highest evaluated temperature, the CO conversion is better reproduced by the model in the case of the reduced catalyst than for the oxidized one (Fig. 2). This could be demonstrating that the reduction of the catalyst prior to the reaction makes difficult the stabilization of the carbonaceous species at higher temperatures as discussed above. The kinetic model does not includes the deactivation of the catalyst by the formation of carbonaceous species, and for that reason there is a better fit of the CO conversion results of the reduced catalyst.

The comparison between the experiment results of the CO oxidation selectivity and the CFD simulations shows some disagreement at temperatures below 200 °C (see Fig. 3). It has to be considered that the CO oxidation selectivity is calculated using the CO and O_2 consumption according to Eq. (2) where CO_{in} and $O_{2_{in}}$ are the flow-rates of CO and O_2 in the feed-stream and CO_{out} and $O_{2_{out}}$ are those at the reactor outlet.

The O_2 consumption included in the denominator of Eq. (2) adds an additional error to the calculation of the CO oxidation selectivity and it might be contributing to the discrepancy between the experimental data and the CFD simulation results. It should be noted that the experimental errors in evaluating the CO and O_2 consumption are higher at low conversions, which could explain the lack of fit with the simulated results at low reaction temperatures. There are other issues that can be also contributing to this result. In this regard, it seems that whereas the kinetic scheme is well established, the kinetic parameters could require some improvement for which a more in depth kinetic study is required.

In view that the CO contents in the feed of the PEMFCs have to be limited to 10–100 ppm, depending on the anode composition, it is interesting to consider the CO content at the outlet of the microchannel reactor, in order to establish if the H_2 has been successfully purified for feeding a fuel cell. The experimental CO concentration at the microchannel outlet is presented in Fig. 6 and it is compared with those obtained by CFD simulations. There is a good correlation between the results that present a minimum CO content between 180 °C and 220 °C. This is indicating that there is an optimal temperature to achieve the maximum CO conversion or the minimum CO emission after the CO-PROX reaction. Moreover, this minimum is close to 10 ppm of CO thus assuring the suitability of the produced H_2 for feeding a PEMFC. On the other hand, the experimental results present a slight shift to higher temperatures with respect to the simulation results. It is expected that the agreement will improve when a refined kinetic model is available.

4. Conclusions

An active CuO_x/CeO_2 coated microreactor was successfully tested on the CO-PROX reaction under a simulated reformate off-gas feed. Prior to the reactions, the catalysts were activated under O_2 or H_2 with no significant differences in activity, obtaining a maximum CO conversion at around 200 °C. As regards the CO oxidation selectivity, the results allowed confirming that the CO conversion is thermodynamically favored against H_2 oxidation at low temperatures. On the other hand, it is found that the presence of CO_2 in the feed inhibits the CO conversion at low temperatures, probably by the formation of carbonaceous species at the catalyst surface.

Finally, a CFD model developed for a microreactor was successfully validated for the first time with experimental catalytic results. The kinetic scheme previously formulated for the CuO_x/CeO_2 powder catalyst was also corroborated. However, complementary studies can be carried out to refine the kinetic parameters included in the model in order to improve the fitting between the experimental and the simulated results.

Acknowledgments

The financial support for this work has been obtained from the Spanish Ministerio de Ciencia e Innovación (ENE2009-14522-C05-01) and (ENE2009-14522-C05-03) cofinanced by FEDER funds from the European Union and from Junta de Andalucía (P09-TEP-5454).

O.H. Laguna and F. Romero-Sarria thank the same Ministry for the FPI fellowship (BES-2007-14409) and the Ramón y Cajal contract awarded respectively.

References

[1] J.O.M. Bockris, Int. J. Hydrogen Energy 33 (2008) 2129–2131.
[2] S. Ahmed, A. Aitani, F. Rahman, A. Al-Dawood, F. Al-Muhaish, Appl. Catal. A: Gen. 359 (2009) 1–24.
[3] J.G. Seo, M.H. Youn, D.R. Park, I. Nam, I.K. Song, Int. J. Hydrogen Energy 34 (2009) 8053–8060.
[4] J.D. Holladay, J. Hu, D.L. King, Y. Wang, Catal. Today 139 (2009) 244–260.
[5] O.H. Laguna, F. Romero Sarria, M.A. Centeno, J.A. Odriozola, J. Catal. 276 (2010) 360–370.
[6] A. Razeghi, A. Khodadadi, H. Ziaei-Azad, Y. Mortazavi, Chem. Eng. J. 164 (2010) 214–220.
[7] F. Mariño, G. Baronetti, M. Laborde, N. Bion, A. Le Valant, F. Epron, D. Duprez, Int. J. Hydrogen Energy 33 (2008) 1345–1353.
[8] N. Bion, F. Epron, M. Moreno, F. Mariño, D. Duprez, Top. Catal. 51 (2008) 76–88.
[9] G. Kolb, V. Hessel, Chem. Eng. J. 98 (2004) 1–38.
[10] X. Ouyang, R.S. Besser, J. Power Sources 141 (2005) 39–46.
[11] G. Kolb, C. Hofmann, M. O'Connell, J. Schürer, Catal. Today 147 (2009) S176–S184.
[12] M. O'Connell, G. Kolb, K.-P. Schelhaas, J. Schuerer, D. Tiemann, A. Ziogas, V. Hessel, Int. J. Hydrogen Energy 35 (2010) 2317–2327.
[13] C.D. Dudfield, R. Chen, P.L. Adcock, J. Power Sources 86 (2000) 214–222.
[14] N.J. Divins, E. López, M. Roig, T. Trifonov, A. Rodríguez, F.G.D. Rivera, L.I. Rodríguez, M. Seco, O. Rossell, J. Llorca, Chem. Eng. J. 167 (2011) 597–602.
[15] T. Glatzel, C. Litterst, C. Cupelli, T. Lindemann, C. Moosmann, R. Niekrawietz, W. Streule, R. Zengerle, P. Koltay, Comput. Fluids 37 (2008) 218–235.
[16] G. Arzamendi, P.M. Diéguez, M. Montes, M.A. Centeno, J.A. Odriozola, L.M. Gandía, Catal. Today 143 (2009) 25–31.
[17] G. Arzamendi, P.M. Diéguez, M. Montes, J.A. Odriozola, E.F. Sousa-Aguiar, L.M. Gandía, Chem. Eng. J. 154 (2009) 168–173.
[18] I. Uriz, G. Arzamendi, E. López, J. Llorca, L.M. Gandía, Chem. Eng. J. 167 (2011) 603–609.
[19] S. Cruz, O. Sanz, R. Poyato, O.H. Laguna, F.J. Echave, L.C. Almeida, M.A. Centeno, G. Arzamendi, L.M. Gandia, E.F. Souza-Aguiar, M. Montes, J.A. Odriozola, Chem. Eng. J. 167 (2011) 634–642.
[20] G. Arzamendi, I. Uriz, P.M. Diéguez, O.H. Laguna, W.Y. Hernández, A. Álvarez, M.A. Centeno, J.A. Odriozola, M. Montes, L.M. Gandía, Chem. Eng. J. 167 (2011) 588–596.
[21] O.H. Laguna, M.A. Centeno, G. Arzamendi, L.M. Gandía, F. Romero-Sarria, J.A. Odriozola, Catal. Today 157 (2010) 155–159.
[22] W.Y. Hernández, M.A. Centeno, F. Romero-Sarria, J.A. Odriozola, J. Phys. Chem. C 113 (2009) 5629–5635.
[23] S. Damyanova, B. Pawelec, K. Arishtirova, M.V.M. Huerta, J.L.G. Fierro, Appl. Catal. A: Gen. 337 (2008) 86–96.
[24] H. Bao, X. Chen, J. Fang, Z. Jiang, W. Huang, Catal. Lett. 125 (2008) 160–167.
[25] P.J. Gellings, H.J.M. Bouwmeester, Catal. Today 12 (1992) 1–101.
[26] P. Avila, M. Montes, E.E. Miró, Chem. Eng. J. 109 (2005) 11–36.
[27] A. Cybulski, J.A. Moulijn, Catal. Rev.: Sci. Eng. 36 (1994) 179–270.
[28] D.M. Frías, S. Nousir, I. Barrio, M. Montes, L.M.T. Martínez, M.A. Centeno, J.A. Odriozola, Appl. Catal. A: Gen. 325 (2007) 205–212.
[29] S.R.J. Saunders, H.E. Evans, M. Li, D.D. Gohil, S. Osgerby, Oxid. Met. 48 (1997) 189–200.
[30] L.C. Almeida, F.J. Echave, O. Sanz, M.A. Centeno, G. Arzamendi, L.M. Gandía, E.F. Sousa-Aguiar, J.A. Odriozola, M. Montes, Chem. Eng. J. 167 (2011) 536–544.
[31] L.C. Almeida, F.J. Echave, O. Sanz, M.A. Centeno, J.A. Odriozola, M. Montes, Stud. Surface Sci. Catal. 175 (2010) 25–33.
[32] W. Liu, M. Flytzanistephanopoulos, J. Catal. 153 (1995) 304–316.
[33] W. Liu, A.F. Sarofim, M. Flytzani-Stephanopoulos, Chem. Eng. Sci. 49 (1994) 4871–4888.
[34] A. Martínez-Arias, M. Fernández-García, O. Gálvez, J.M. Coronado, J.A. Anderson, J.C. Conesa, J. Soria, G. Munuera, J. Catal. 195 (2000) 207–216.
[35] O. Pozdnyakova, D. Teschner, A. Wootsch, J. Kröhnert, B. Steinhauer, H. Sauer, L. Toth, F.C. Jentoft, A. Knop-Gericke, Z. Paál, R. Schlögl, J. Catal. 237 (2006) 1–16.
[36] X. Ouyang, R.S. Besser (Eds.), CO Clean-up: Preferential Oxidation, Willey-VCH Verlag, Wenheim, 2009.